

Divergence-free algorithms for moment-thrust-curvature analysis of arbitrary sections

Liang Chen^a, Si-Wei Liu^{*} and Siu-Lai Chan^b

Department of Civil and Environmental Engineering,
The Hong Kong Polytechnic University, Hong Kong, China

(Received January 06, 2017, Revised July 05, 2017, Accepted July 12, 2017)

Abstract. Moment-thrust-curvatures (M-P- Φ curves) are fundamental quantities for detailed descriptions of basic properties such as stiffness and strength of a section under axial loads required for accurate computation of the deformations of reinforced concrete or composite columns. Currently, the finite-element-based methods adopting small fibers for analyzing a section are commonly used for generating the M-P- Φ curves and they require large amounts of computational time and effort. Further, the conventional numerical procedure using the force-control method might encounter divergence problems under high compression or tension. Therefore, this paper proposes a divergence-free approach, combining the use of the displacement-control and the Quasi-Newton scheme in the incremental-iterative procedure, for generating the M-P- Φ curves of arbitrary sections. An efficient method for computing the strength from concrete components is employed, where the stress integration is executed by layer-based algorithms. For easy modeling of residual stress, cross sections of structural steel components are meshed into fibers for strength resultants. The numerical procedure is elaborated in detail with flowcharts. Finally, extensive validating examples from previously published research are given for verifying the accuracy of the proposed method.

Keywords: composite; steel; section; numerical; concrete; moment-curvature analysis

1. Introduction

Moment-thrust-curvature relations (M-P- Φ curve) are basic properties for stiffness, strength and ductility of a section under compressions or tensions, which are required for an accurate calculation of member deformations and flexural rigidities. Due to the variability in the material characteristics of concrete and steel, the behaviours of the sections with or without concrete under axial loads are significantly different. For an illustration in Fig. 1, the concrete in an encased composite section would be easily cracked under tension, and therefore, a low-level compression force might increase the strength as well as the rigidity of the section with concrete material. Due to the isotropic properties of steel, the flexural stiffness of a steel section is not affected by compression or tension forces (see Fig. 2), whilst the levels of axial loads will reduce its moment resistance capacities. Conceptual summaries on the influences of compressions or tensions to the behaviours of reinforced-concrete, composite and structural steel sections are given in Tables 1 and 2.

Moment-thrust-curvature relations are essential for a successful design of concrete structures for the estimations

and the calculations for stiffness and strength of sections, respectively. For example, the member deformations can be calculated by the curvature at the most critical location along its length according to Eurocode 2-1-1(2004); and the rigidity can be determined with aid of M-P- Φ curves by referring to the applied loads as studied by Avşar *et al.* (2014) and Caglar *et al.* (2015). Further, these relations are usually used for evaluating the energy dissipation capacity or ductility of a section in the modern seismic design method based on the performance-based approach (Sato *et al.* 2002, Oller and Barbat 2006). M-P- Φ curves are fundamental quantities for the frame analysis using distributed-plasticity elements via force-based approaches (Spacone *et al.* 1996, Neuenhofer and Filippou 1997, Neuenhofer and Filippou 1998, De Souza 2000, Ngo-Huu and Kim 2012) and plastic zone methods (Clarke 1994, Teh and Clarke 1999, Jiang *et al.* 2002), where the fiber-based section model (i.e., Fig. 2(a)) is required during the incremental-iterative procedure resulting in large computational time. As reported by Kwak and Kim (2002), when adopting the pre-generated M-P- Φ curves, this finite-element-based analysis method can be eliminated and dramatically improves the numerical efficiency. To this, there is a need for an efficient and reliable approach for generating the moment-thrust-curvature relations of arbitrary sections for both design and analysis.

The related research on generating the M-P- Φ curves initiated in 1960s Fukumoto (1963) proposed a computational procedure for determining the moment-thrust-curvature relationships of steel wide-flange sections. Burns (1964) investigated the curvatures under bending moments for the partially pre-stressed concrete beams. Hsu

*Corresponding author, Research Fellow,

E-mail: siwei.liu@connect.polyu.hk

^a Research Assistant,

E-mail: liang.chen@polyu.edu.hk

^b Chair Professor,

E-mail: ceslchan@polyu.edu.hk

(1966) studied the moment-curvature relations for the beams with nonlinear material properties via numerical algorithms. Recently, researchers including Sato *et al.* (2002), El-Tawil *et al.* (1999), Varma *et al.* (2002), Chiorean (2010), Charalampakis and Koumoussis (Charalampakis and Koumoussis), Chadwell and Imbsen (2004), adopted the fiber-based section model (i.e., Fig. 3(a)) for generating moment-thrust-curvatures, and the section needs to be decomposed into large numbers of small fibers for the numerical accuracy. Herein, an efficient modeling scheme is proposed, as indicated in Fig. 3(b), where the concrete components are automatically meshed into a series of parallel layers, and the structural steel components are meshed into triangle fibers for an easy incorporation of residual stresses.

Alternatively, several close-formed expressions for typical sections were proposed by for improving the efficiency of moment-curvature analysis. Duan *et al.* (1993) develop a set of mathematical M-P- Φ expressions for dented and undented steel tubular sections under combined multidirectional bending and axial load. Soranakom and Mobasher (2007) present a closed-form solution for the moment-curvature response of cement-based composites with homogeneously distributed reinforcement. Monti and Petrone (2015) propose analytical equations for the calculation of the yield and ultimate moments, and the curvatures for RC sections subjected to the axial forces. Whereas these methods are only applicable for analyzing some typical sections with idealized material properties, and cannot cover all the design cases in practice (i.e., Fig. 4). Thereby, a general analysis method is proposed in this paper for all types of sections to remedy the constraint.

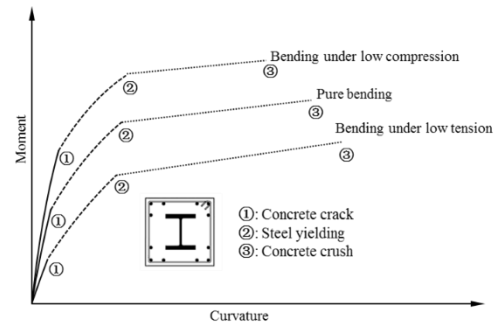


Fig. 1 Moment-thrust-curvature relations of composite section

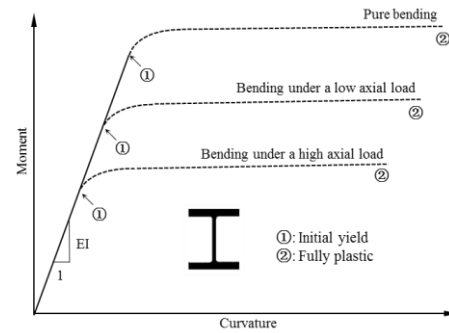


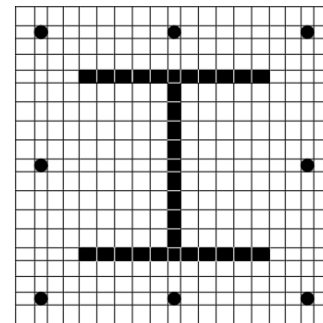
Fig. 2 Moment-thrust-curvature relations of steel section

Table 1 Conceptual influences of axial loads to RC and composite section

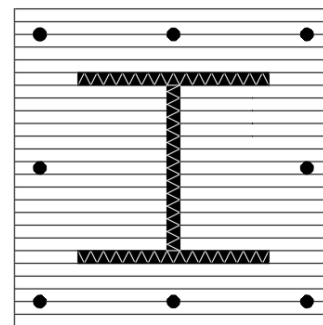
		Compression	Tension
Moment Capacity	Flexural rigidity	↑	↓
	Concrete crack	↑	↓
	Steel yielding	↑	↓
Curvature	Concrete crush	↑	↓
	Concrete crack	↑	↓
	Steel yielding	↑	↓
		↓	↑

Table 2 Conceptual influences of axial loads to structural steel section

		Compression	Tension
Flexural rigidity		-	-
Moment Capacity	Initial yield	↓	↓
	Fully yield	↓	↓
Curvature	Initial yield	↓	↓
	Fully yield	↓	↓



(a) Fiber-based model



(b) Proposed model

Fig. 3 Proposed Fiber-based models

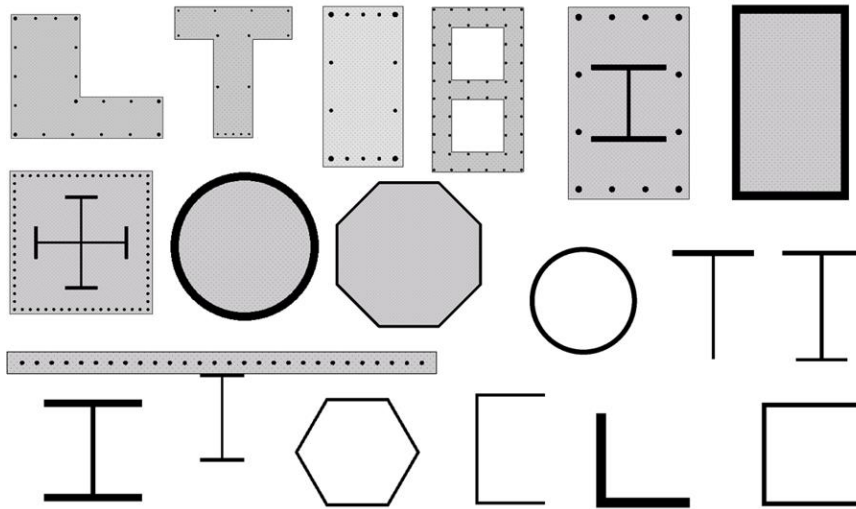


Fig. 4 Common types of sections

In this paper, a divergence-free approach combining the use of the displacement-control and the Quasi-Newton scheme in the incremental-iterative procedure to generate the M-P- Φ curves of arbitrary steel, concrete and composite section is proposed. The section modeling method via components is introduced. An efficient algorithm for computing the strength from the concrete components is employed, where the stress integrations are executed by layer-based model. Structural steel components are meshed into fibers for easy modeling of residual stress. The numerical procedure is elaborated in detail with the aid of flowcharts. Finally, several examples from available literatures are given for validating the accuracy of the proposed method.

2. Assumptions and definitions

In the present study, the following assumptions are adopted:

- Plane sections remain plane after deformation (Euler-Bernoulli hypothesis). Consequently, the strain change linearly along the depth of the cross-section.
- Full strain compatibility is assumed between the steel and the surrounding concrete which implies that the bond-slip between the concrete and steel is negligible.
- Local buckling of steel plates is prevented and is not considered its influence on the material strength.
- Steel reinforcement embedded in concrete does not buckle under compressions.
- Compressive stresses and strains are taken to be positive.
- The effect of concrete cracking or crushing on the torsional stiffness is out of the scope of this study.

3. Section modeling via components

For describing arbitrary types of cross sections, a component-based modeling method is formulated, with four basic types of components employed namely as structural steel, reinforcement, concrete and opening. A schematic decomposition of a composite section via components is presented in Fig. 5. The concrete components are stored as groups of coordinates of vertices and will be dynamically divided into parallel-layers during the iterative procedure. The steel components are automatically meshed into a series of triangular fibers, while the reinforcement components are treated as point elements with small occupied region equaling to the bar area. The opening components are only allowed to be established over the concrete components, and described by groups of coordinates of vertices.

Three sets of coordinate systems, namely ZCY , zoy and uov shown in Fig. 6 are established. The ZCY axis is global and to describe all the components. The $yozy$ system is the intermediate axis with the origin as the geometric centroid of the cross-section referring to the ZCY axis. The uov system is the load-reference system and the u -axis of this system is parallel to the neutral axis. This system shares the same origin as the geometric centroid of the cross-section with the zoy system. And the axes of zoy system are parallel to the axes of ZCY system. The geometric centroid of a section can be computed as

$$Z_{gc} = \frac{\sum_{i=1}^{n_c} A_{c_i} Z_{c_i} + \sum_{i=1}^{n_s} A_{s_i} Z_{s_i} + \sum_{i=1}^{n_r} A_{r_i} Z_{r_i} - \sum_{i=1}^{n_o} A_{o_i} Z_{o_i}}{\sum_{i=1}^{n_c} A_{c_i} + \sum_{i=1}^{n_s} A_{s_i} + \sum_{i=1}^{n_r} A_{r_i} - \sum_{i=1}^{n_o} A_{o_i}} \quad (1)$$

$$Y_{gc} = \frac{\sum_{i=1}^{n_c} A_{c_i} Y_{c_i} + \sum_{i=1}^{n_s} A_{s_i} Y_{s_i} + \sum_{i=1}^{n_r} A_{r_i} Y_{r_i} - \sum_{i=1}^{n_o} A_{o_i} Y_{o_i}}{\sum_{i=1}^{n_c} A_{c_i} + \sum_{i=1}^{n_s} A_{s_i} + \sum_{i=1}^{n_r} A_{r_i} - \sum_{i=1}^{n_o} A_{o_i}} \quad (2)$$

in which, n_c , n_s , n_r and n_o are the numbers of concrete components, steel components, reinforcements and openings, respectively.

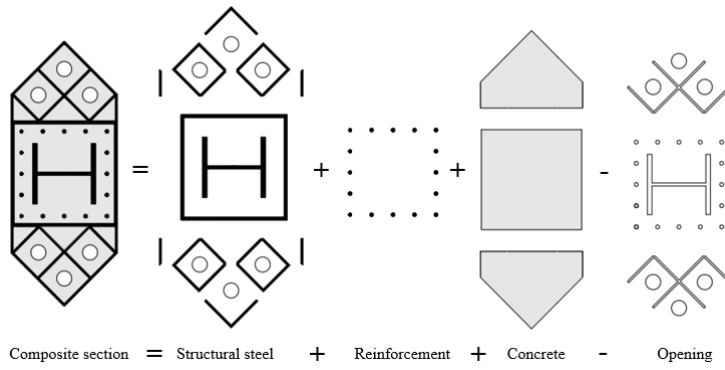


Fig. 5 The component-based modeling method

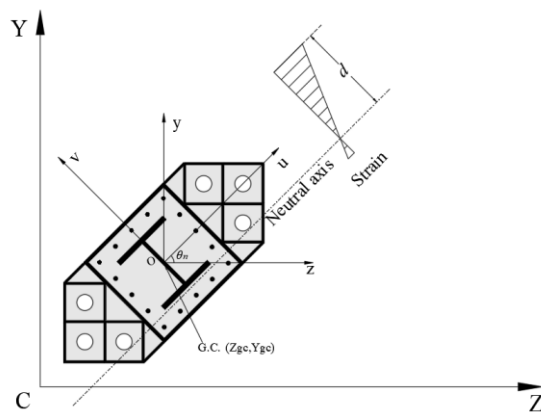


Fig. 6 Coordinate systems

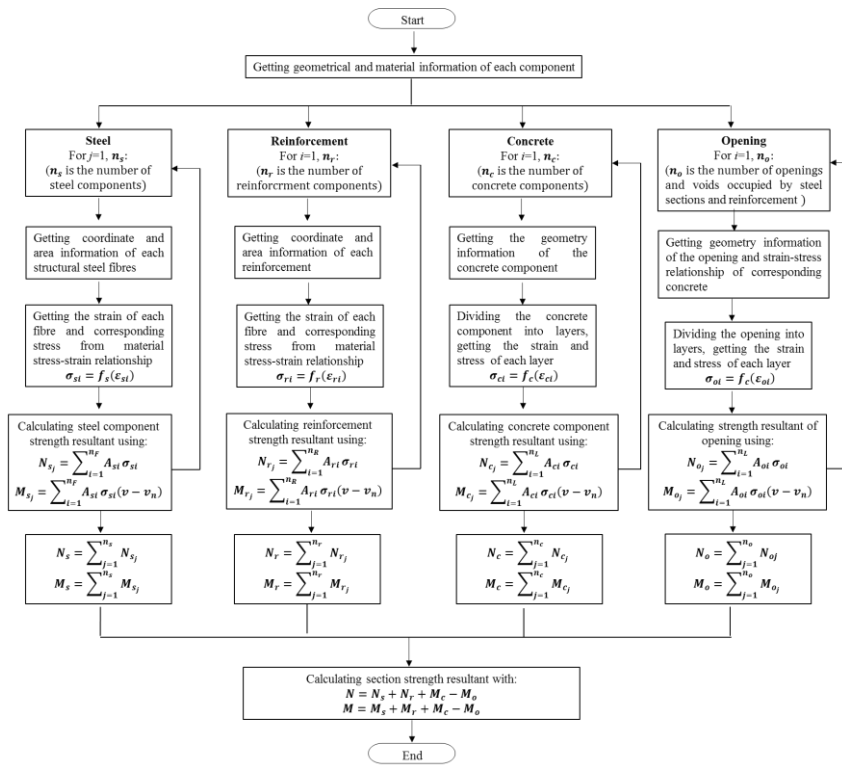


Fig. 7 Procedure of stress integrations for the components

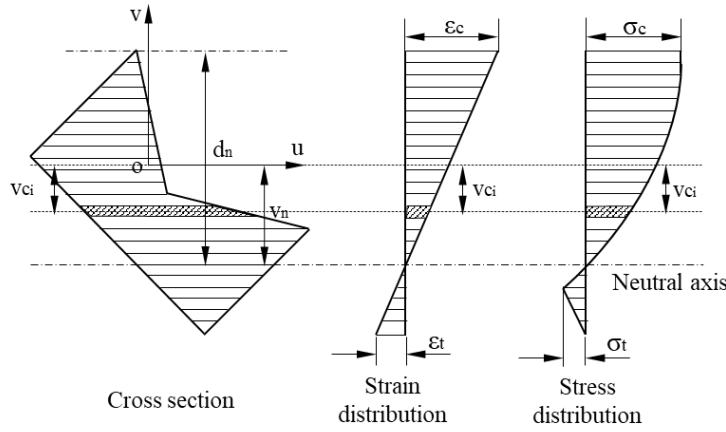
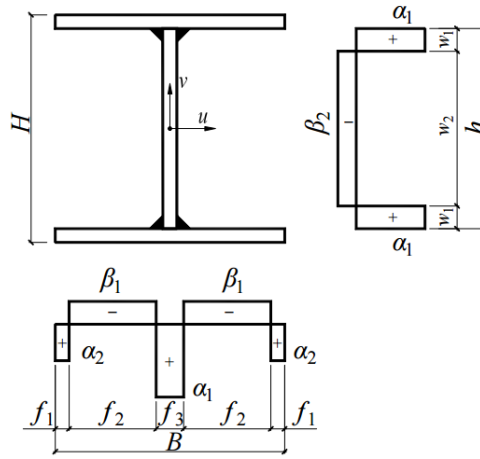


Fig. 8 Layer-based integration method


 Fig. 9 Residual stress distribution pattern by Li *et al.* (2015)

The coordinates among these coordinate systems can be transferred by the following operations

$$\begin{Bmatrix} z \\ y \end{Bmatrix} = \begin{Bmatrix} Z \\ Y \end{Bmatrix} - \begin{Bmatrix} Z_{gc} \\ Y_{gc} \end{Bmatrix} \quad (3)$$

$$\begin{Bmatrix} u \\ v \end{Bmatrix} = \begin{Bmatrix} \cos\theta_n & \sin\theta_n \\ -\sin\theta_n & \cos\theta_n \end{Bmatrix} \begin{Bmatrix} z \\ y \end{Bmatrix} \quad (4)$$

where, θ_n denote for the inclined angle between the uov and zoy coordinate systems.

4. Stress integration algorithms

The whole sectional strengths, in terms of axial resistance N and bending moment M , can be calculated by integration of stresses within the components, where the detailed procedure is given in Fig. 7. Due to the characteristics in the varied types of components, i.e. steel, reinforcement, concrete and opening components, the resultant strengths are separately calculated via these components and the total strength of the section is then computed by

$$N = N_s + N_r + (N_c - N_o) \quad (5)$$

$$M = M_s + M_r + (M_c - M_o) \quad (6)$$

where N_s , N_r , N_c and N_o are the axial resistances from the steel, the reinforcement, the concrete and the opening components, respectively; and M_s , M_r , M_c and M_o are the moment resistances from the steel, the reinforcement, the concrete and the opening components, respectively.

The basic assumption in the Euler-Bernoulli hypothesis is the strain along the direction perpendicular to the neutral axis is proportional to the distance from the axis. Therefore, an efficient approach using layers instead of fibers for the stress integration is proposed, where the components are divided into series of layers as indicated in Fig. 8. A similar concept for the stress resultant is also adopted by Liu *et al.* (2012).

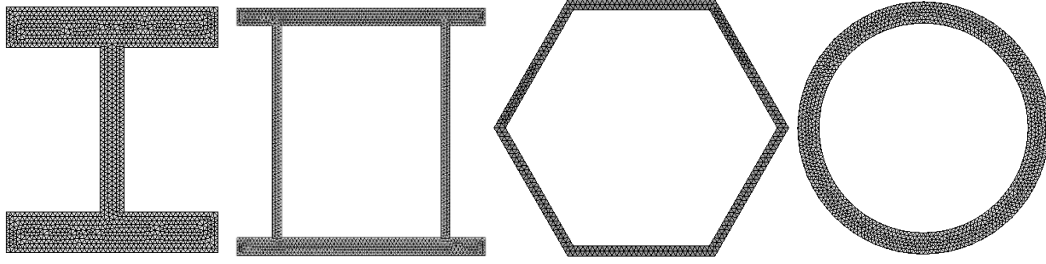


Fig. 10 Steel sections meshed using the algorithm by Niceno (2002)

However, the residual stresses, as illustrated in Fig. 9, in the steel plate could significantly affect the initial yield moment of structural steel sections as reported by Li *et al.* (2015), which need to be considered in the analysis. To this, the steel sections are meshed into small fibers for direct considerations of residual stress although increasing the computing time. The algorithm proposed by Niceno (2002) (see Fig. 10) is introduced for generating the mesh-grids for any irregular or regular steel sections.

Therefore, two schemes of stress integration algorithms, i.e. the layer-based and the fiber-based methods, are proposed. The former approach is applied for calculating the strengths of the concrete and opening components, while the latter method is used for computing the forces among the steel fibers and reinforcement components.

4.1 Layer-based integration method for concrete and openings components

The concrete and open components will be dynamically divided into layers at each time when the neutral axis is known (see Fig. 8). These layers are parallel to the neutral axis, where the strains are assumed to be constant within each layer. From our numerical experience, the height of each layer is 1% of the section height for an accurate analysis result in engineering practice. The stress within the layer is taken as $f(\varepsilon_i)$, where the ε_i is the strain at the middle height of the layer and f is the function for stress versus strain relations of the material.

The strength resistance of the i^{th} layer in the j^{th} concrete component are computed by

$$\begin{aligned} N_{ci}^j &= \int_{u_i} \int_{v_i} f_c^j(\varepsilon) dudv \\ &= f_c^j(\varepsilon_{ci}^j) \int_{u_i} \int_{v_i} dudv = f_c^j(\varepsilon_{ci}^j) A_{ci} \end{aligned} \quad (7)$$

$$\begin{aligned} M_{ci}^j &= \int_{u_i} \int_{v_i} f_c^j(\varepsilon)(v - v_n) dudv \\ &= f_c^j(\varepsilon_{ci}^j)(v_{ci} - v_n) \int_{u_i} \int_{v_i} dudv \\ &= f_c^j(\varepsilon_{ci}^j)(v_{ci} - v_n) A_{ci} \end{aligned} \quad (8)$$

$$A_{ci} = \frac{1}{2} \left| \sum_{i=1}^{n-1} (u_i v_{i+1} - u_{i+1} v_i) + (u_n v_1 - u_1 v_n) \right| \quad (9)$$

in which A_{ci} is the area of the i^{th} layer; and v_{ci} and v_n are the v-coordinates of the center line and the neutral axis in uov axis.

The strength resistances of each component can be calculated by

$$N^j = \int_u \int_v f^j(\varepsilon) dudv = \sum_{i=1}^{n_L} N_i^j \quad (10)$$

$$M^j = \int_u \int_v f^j(\varepsilon)(v - v_n) dudv = \sum_{i=1}^{n_L} M_i^j \quad (11)$$

in which n_L is the number of layers.

The detailed calculation procedure is illustrated in Fig. 11, and the openings and voids occupied by steel components and reinforcements will be removed by the negative area approach (Liu *et al.* 2012).

4.2 Fiber-based integration method for steel and reinforcement components

The structural steel components are meshed into fibers before the commencement of the numerical procedure, where the robust algorithm proposed by Niceno (2002) is employed for generating mesh-grids for arbitrary steel sections.

The stress resultant of the j^{th} steel component can be computed as

$$N_s^j = \int_u \int_v f_s^j(\varepsilon) dudv = \sum_{i=1}^{n_F} A_{si}^j f_s^j(\varepsilon_{si}^j) \quad (12)$$

$$M_s^j = \int_u \int_v f_s^j(\varepsilon)(v - v_n) dudv = \sum_{i=1}^{n_F} A_{si}^j f_s^j(\varepsilon_{si}^j) (v_{si}^j - v_n) \quad (13)$$

in which A_{si}^j is the area of the i^{th} fiber of the j^{th} steel component; v_{si}^j is the v-coordinate of the fiber centroid in the uov axis; and n_F is the number of fibers.

Similarly, each reinforcing bar can be treated as a special type of steel fiber, and the strength resistance from the j^{th} reinforcement component is calculated by

$$N_r^j = \sum_{i=1}^{n_R} A_{ri}^j f_r^j(\varepsilon_{ri}^j) \quad (14)$$

$$M_r^j = \sum_{i=1}^{n_R} A_{ri}^j f_r^j(\varepsilon_{ri}^j) (v_{ri}^j - v_n) \quad (15)$$

in which A_{ri}^j is the area of the i^{th} reinforcing bar of the j^{th} reinforcement component; v_{ri}^j is the v-coordinate of the bar centroid in the uov axis; and n_R denote the number of bars.

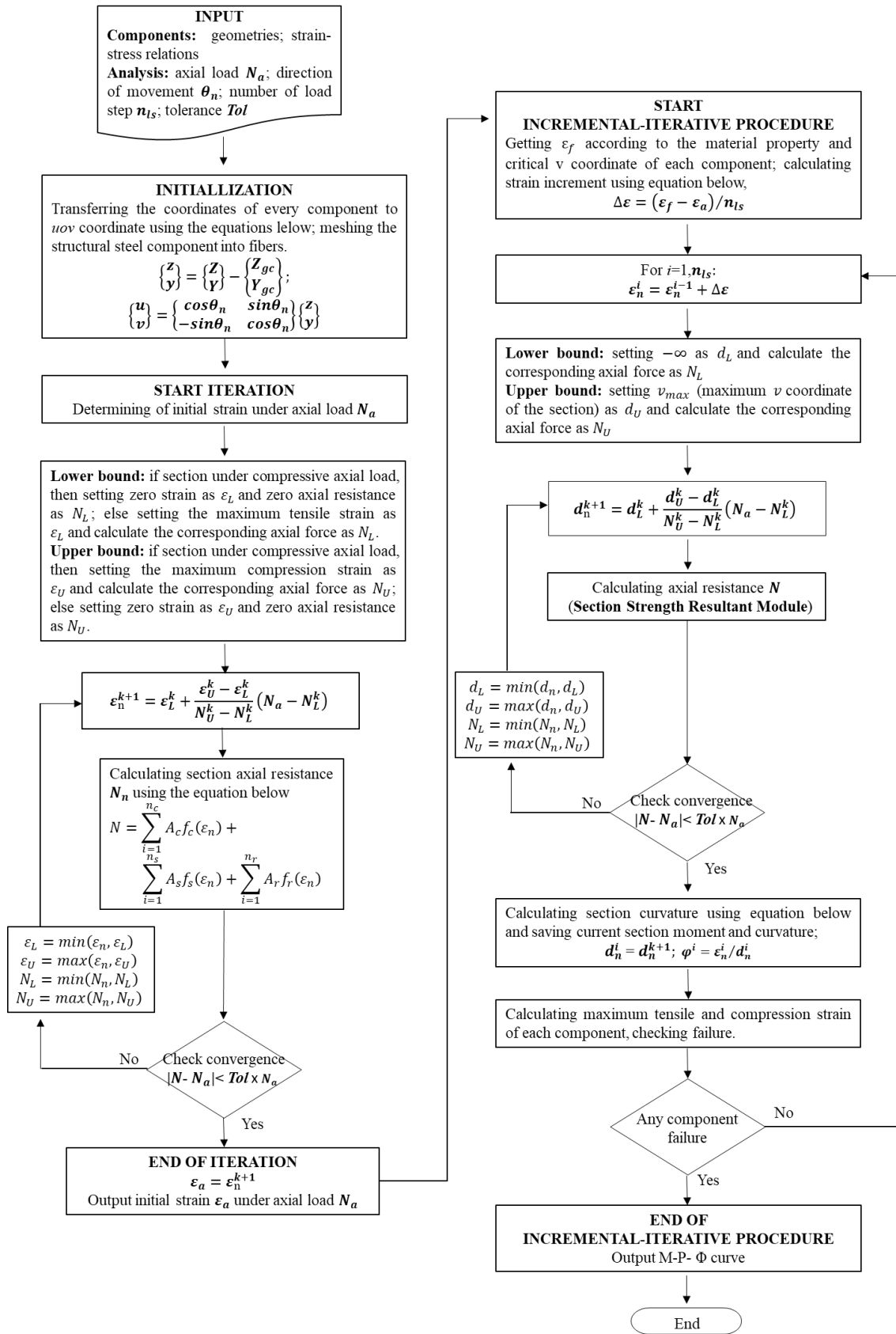


Fig. 11 Flowchart of the numerical analysis

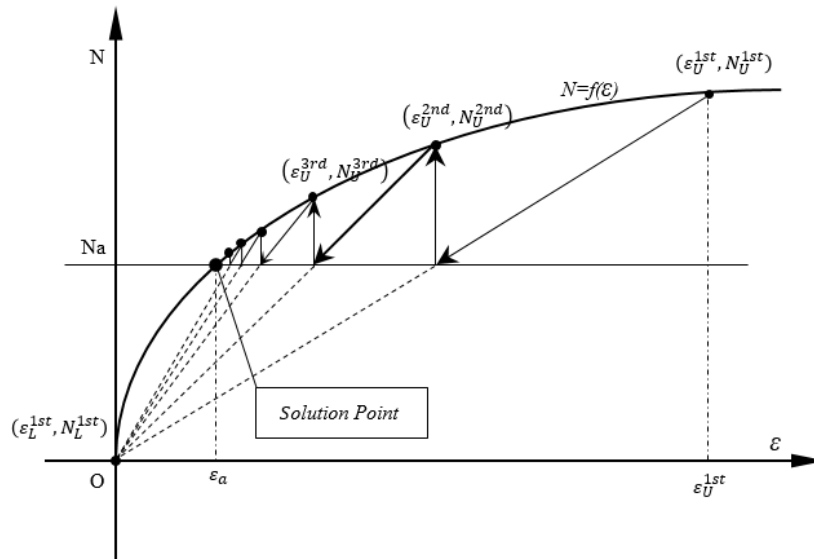


Fig. 12 Divergence-free Quasi-Newton iteration scheme for ϵ_α

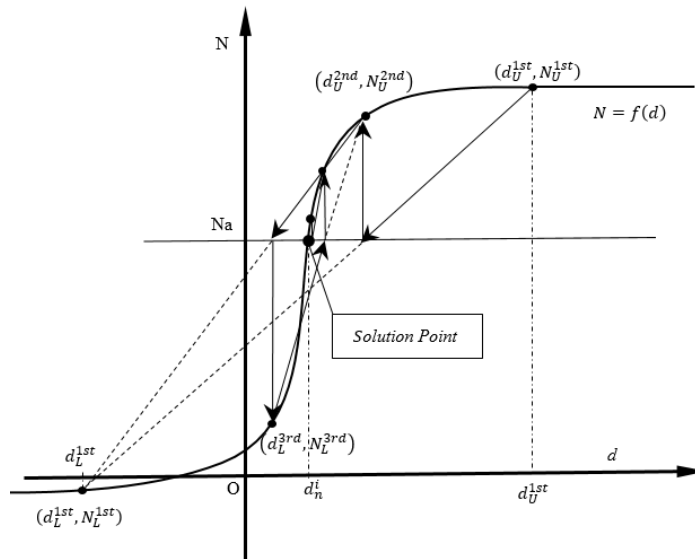


Fig. 13 Divergence-free Quasi-Newton iteration scheme for d_α

5. Numerical procedure for the moment-thrust-curvatures analysis

The detailed flowchart of analysis is shown in Fig. 11, where the displacement-based method and the Quasi-Newton approach are used for the incremental and the iterative procedures, respectively. The initial axial strain of the section under the applied axial load should be determined first, and the strain at the topmost of the section is then increased till the failure value is reached. The location of neutral axis is determined at every strain increment and the corresponding curvature and the corresponding moment resistance is computed.

The initial axial strain of the section under the applied axial is calculated via the Quasi-Newton iterative procedure as illustrated in Fig. 12. This procedure is unconditionally stable when the lower and the upper bounds are properly assumed at the 1st iteration. Fig. 11 shows that, the boundaries are determined by assuming the strains as zero and maximum fracture value for the lower and the upper bounds respectively and the iteration can be executed via the following equation

$$\epsilon_n^{k+1} = \epsilon_L^k + \frac{\epsilon_U^k - \epsilon_L^k}{N_U^k - N_L^k} (N_a - N_L^k) \tag{16}$$

in which ϵ_n is the updated strain of the section; ϵ_L and ϵ_U are the strains of the section with the resistances being smaller

and greater than the applied axial force respectively; and N_L and N_U are the axial resistances calculated by ε_L and ε_U , respectively. The lower bound and upper bound of the above iterative procedure are defined as:

- **Lower bound:** if the section under compressive axial load, then setting zero strain as ε_L and zero axial resistance as N_L ; else setting the maximum tensile strain as ε_L and calculate the corresponding axial force as N_L .
- **Upper bound:** if the section under compressive axial load, then setting the maximum compression strain as ε_U and calculate the corresponding axial force as N_U ; else setting zero strain as ε_U and zero axial resistance as N_U .

The similar iteration algorithm is proposed for computing the location of the neutral axis as shown in Fig. 13. The implicit function between the axial resistance N and the location of the neutral axis “ d ” is established, and a Quasi-Newton iterative method is proposed for finding the position of the d with respect to the applied N_a via the following equation

$$d_n^{k+1} = d_L^k + \frac{d_U^k - d_L^k}{N_U^k - N_L^k} (N_a - N_L^k) \quad (17)$$

in which d_n is the updated depth of the neutral axis; d_L is the neutral axis depth with the axial resistance N_L smaller than the applied axial force and d_U is the neutral axis depth with the axial resistance N_U greater than the applied axial force. The lower bound and upper bound of this iterative procedure are defined as:

- **Lower bound:** setting $-\infty$ as d_L and calculate the corresponding axial force as N_L .
- **Upper bound:** setting v_{max} (maximum v coordinate of the section) as d_U and calculate the corresponding axial force as N_U .

The above iterative procedures are divergence-free only since the lower and the upper bounds are properly determined.

Once the depth of the neutral axis d_n is determined at every strain increment at the topmost of the section, the moment resistance can be computed using the stress integration method in Fig. 7 and the curvature can be calculated by

$$\varphi^i = \varepsilon_n^i / d_n^i \quad (18)$$

where ε_n^i is the strain at the i^{th} step, which increases from the strain under applied axial force ε_a by $\Delta\varepsilon$ at each load step during the incremental procedure and calculated by the following equation.

$$\Delta\varepsilon = (\varepsilon_f - \varepsilon_a) / n_{ls} \quad (19)$$

in which n_{ls} denote the number of load steps; and ε_f is the fracture strain.

The fracture of any components in the section is checked during each load step. When one of the components is loaded to exceed its failure curvature, the analysis procedure will be terminated and the corresponding moment resistance is then being taken as the ultimate moment capacity.

6. Verification examples

The proposed divergence-free numerical method for generating M-P- Φ curves is applicable to arbitrary steel, reinforced-concrete and composite sections. In order to examine its accuracy and validity, several examples from literatures are studied as follows. In these examples, the concrete component are divided into 100 layers and the convergence tolerance is 0.1%.

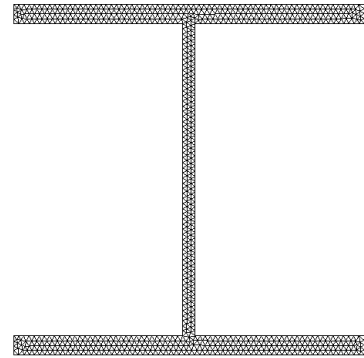
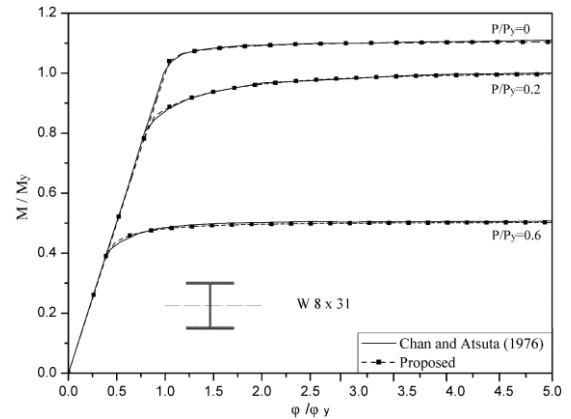
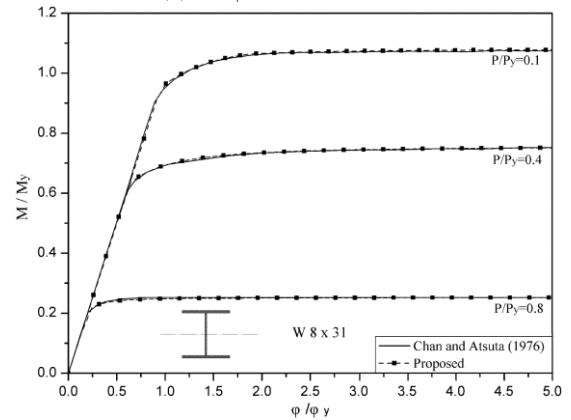


Fig. 14 Fiber mesh of W8x31 section



(a) $P/P_y = 0, 0.2$ and 0.6



(b) $P/P_y = 0.1, 0.4$ and 0.8

Fig. 15 Comparisons for the moment-thrust-curvatures of W8x31 section

A structural steel section under a series of axial loads originally studied by Chen and Atsuta (1976) using the closed-form expressions is studied analyzed in this example.

The section is W8x31 wide-flange of height and width both 203 mm. The thicknesses of web and flange plates are respectively 7 mm and 11 mm. Bi-linear constitutive model is assumed for the steel material, and the Young's modulus is 200 GPa. A total of 1478 fiber elements are generated by the meshing algorithm (Niceno 2002), as shown in Fig. 14, for constructing the steel section in the analysis. The moment curvatures under six axial loads, e.g., 0, 0.1P_y, 0.2P_y, 0.4P_y, 0.6P_y and 0.8P_y, are generated, where P_y denote the cross sectional capacity.

The analysis results using the closed-form solutions by Chen and Atsuta (1976) are employed as benchmarks, and the comparisons results between the proposed method and by Chen and Atsuta (1976) are plotted in in Fig. 15, where the M_y and φ_y are the initial yield moment and the initial yield curvature, respectively. From the comparisons, the M-P-Φ curves generated by the proposed algorithm are identical to those by the closed-form expressions and the accuracy and reliability of the numerical procedure are confirmed in this pure steel section example.

6.2 Reinforced-concrete sections by Simão et al. (2016)

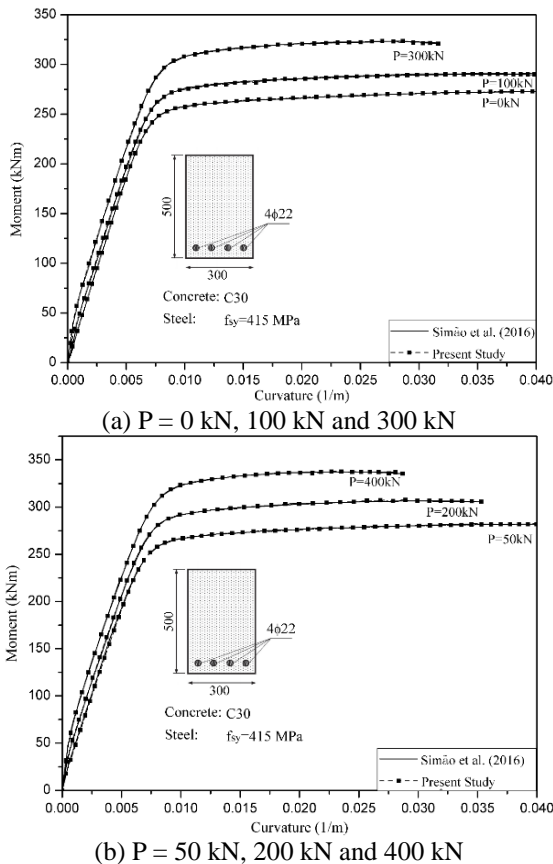


Fig. 16 Comparisons for the moment-thrust-curvatures of the RC section with tensile reinforcement only

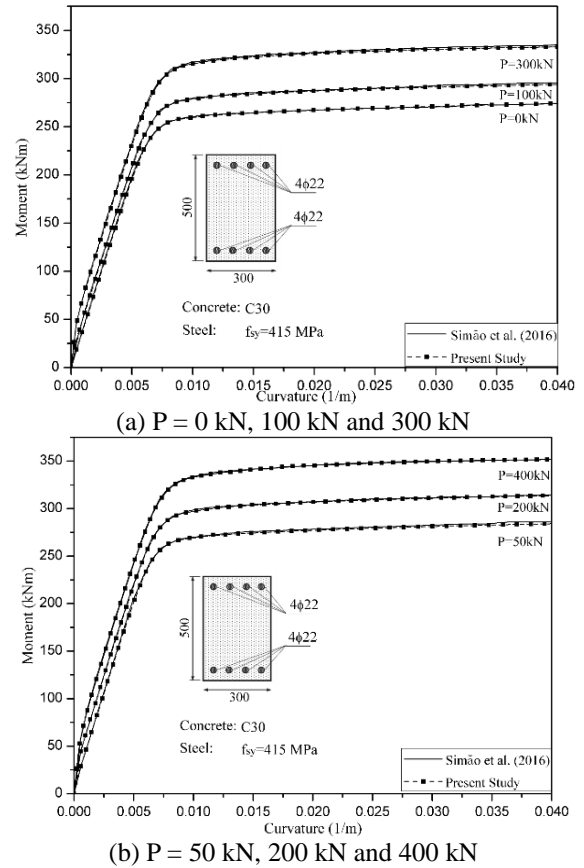


Fig. 17 Comparisons for the moment-thrust-curvatures of a RC section with tensile and compression reinforcement

A series of closed-form expressions for generating the M-P-Φ curves for the rectangular reinforced concrete sections is proposed by Simão et al. (2016). In this example, two types of concrete sections, i.e., singly and doubly reinforced, are analyzed and compared with the results by the closed-form solutions (Simão et al. 2016). The width and height of the section are 300 mm and 500 mm, respectively, and the cover is 50 mm. The concrete grade is C30 and the yield strength of reinforcement is 415 MPa.

The moment versus curvatures under the six levels of axial compressions, i.e., 0 kN, 50 kN, 100 kN, 200 kN, 300 kN and 400 kN, are generated by the proposed method and the hand calculation methods by Simão et al. (2016).

The comparison results are plotted in Figs. 16 and 17 for the singly and the doubly reinforced concrete sections, respectively, where the curvatures ranged from 0 to 0.04 are generated. The analyzed M-P-Φ curves by the proposed numerical approach are almost the same as the closed-form expressions, showing the high accuracy in tracing the section behaviors with nonlinear material properties.

6.3 Rectangular concrete-filled composite section by Uy (2001)

This example employs a rectangular concrete-filled composite section for validation, which was originally tested by Uy (2001) and later studied by Gayathri et al. (2004) using the fibre-based method. The length and width of the cross-

section are both 160 mm. The thickness of the steel tube is 5 mm and has been meshed into fibers as shown in Fig. 18(a).

The cube strength of concrete is 30 MPa, while the yield strength of steel tube is 770 MPa.

The analysis results by the proposed method are plotted and compared with those by experiment (Uy 2001) and by the fiber-based analysis approach (Gayathri *et al.* 2004) as illustrated in Fig. 18(b). Both the elastic behaviours and the ultimate moment resistances can be accurately predicted using the numerical algorithms in this paper when compared with the experimental results (Uy 2001), where the slight differences in the elasto-plastic range is due to the nonlinear concrete properties in the tri-axial loading state.

6.4 Encased composite section by El-Tawil and Deierlein (1999)

An encased composite section is investigated in this example which was studied by El-Tawil and Deierlein (1999) using the finite-element method (FEM). The section is rectangular with width and height equal to 700 mm with the section being W14x211. This encased steel section is meshed into 2050 fibers as shown in Fig. 19(a). The yield strengths of reinforcement and structural steel are 414 MPa and 345 MPa, respectively. There is twelve reinforcing bars in the cross section. Three concrete grades with the cube strength of 28 MPa, 69 MPa and 110 MPa are considered.

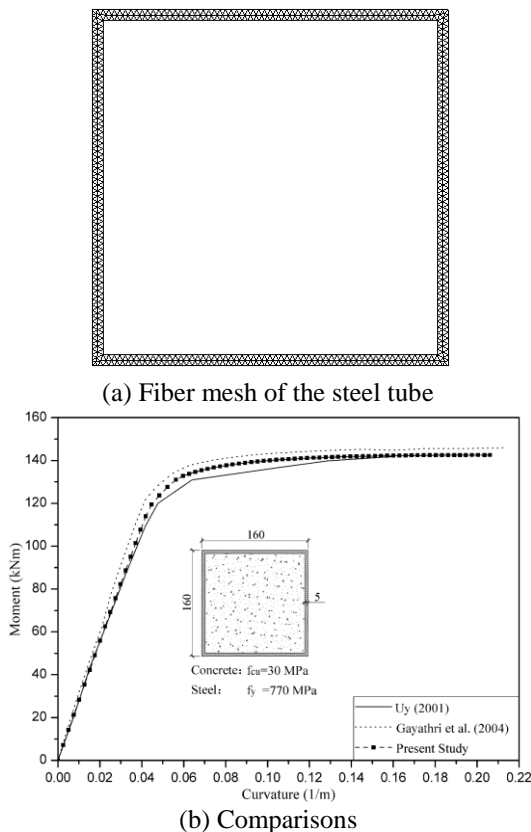


Fig. 18 Moment-curvatures of a rectangular concrete filled section

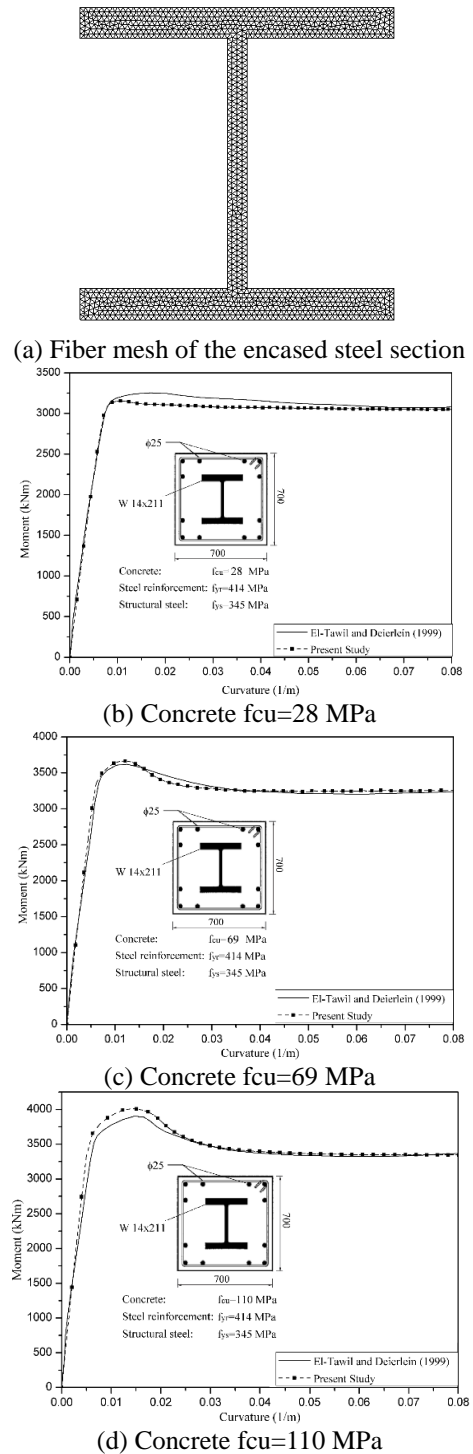


Fig. 19 Comparisons for the moment -curvatures of a rectangular encased composite section

The moments versus curvatures for this section with different grades of concrete are generated and shown in Figs. 19(b)-19(d), where the results by the FEM (El-Tawil and Deierlein 1999) are compared. From Fig. 19, the moment-curvatures can be accurately reproduced by the proposed numerical method regardless of grades of concrete when compared with the sophisticated but less computationally efficient FEM.

7. Conclusions

Moment-thrust-curvatures (M-P- Φ curves) can comprehensively reflect the basic properties as stiffness and strength of a section under axial loads, which are necessary for an accurate determination of member deformations and flexural rigidities. This paper proposes a divergence-free approach, combining the displacement-control and the Quasi-Newton scheme in the incremental-iterative procedure, for generating the M-P- Φ curves of arbitrary steel, concrete and composite sections. A section modeling method using varied types of components as concrete, structural steel, reinforcement and openings, is introduced for describing any types of sections. An efficient algorithm for computing the strength from the concrete components is adopted, where the stress integrations are executed by layer-based approaches. The numerical procedure is elaborated in detail with flowcharts. Finally, several examples from available literatures are compared for validating the accuracy of the proposed method.

Acknowledgments

The authors are grateful to the financial supports by the Research Grant Council of the Hong Kong SAR Government on the project “Second-order and Advanced Analysis of Arches and Curved Structures (PolyU 152012/14E)” and “Second-Order Analysis of Flexible Steel Cable Nets Supporting Debris (PolyU 152008/15E)” and support by Innovation and Technology Fund of the Hong Kong SAR Government for the project “Development of an energy absorbing device for flexible rock-fall barriers (ITS/059/16FP)” and by the Hong Kong Branch of Chinese National Engineering Research Centre for Steel Construction of The Innovation and Technology Fund of the Hong Kong SAR Government for the project “Advanced Numerical Analysis for Building Structures using High Performance Steel Materials”

References

- Avşar, Ö., Bayhan, B. and Yakut, A. (2014), “Effective flexural rigidities for ordinary reinforced concrete columns and beams”, *Struct. Des. Tall Spec. Build.*, **23**(6), 463-482.
- Burns, N.H. (1964), “Moment curvature relationships for partially prestressed concrete beams”, *PCI J.*, **9**(1), 52-63.
- Caglar, N., Demir, A., Ozturk, H. and Akkaya, A. (2015), “A simple formulation for effective flexural stiffness of circular reinforced concrete columns”, *Eng. Appl. Artif. Intel.*, **38**, 79-87.
- Chadwell, C.B. and Imbsen, R.A. (2004), “XTRACT: A tool for axial force - ultimate curvature interactions”, *Structures*, **2004**, 1-9.
- Charalampakis, A.E. and Koumoussis, V.K. (2008), “Ultimate strength analysis of composite sections under biaxial bending and axial load”, *Adv. Eng. Softw.*, **39**(11), 923-936.
- Chen, W.F. and Atsuta, T. (1976), *Theory of Beam-Columns, Volume 1: In-Plane Behaviour and Design*, J Ross Publishing Classics, New York, NY, USA.
- Chiorean, C. (2010), “Computerised interaction diagrams and moment capacity contours for composite steel-concrete cross-sections”, *Eng. Struct.*, **32**(11), 3734-3757.
- Clarke, M. (1994), “Plastic-zone analysis of frames”, *Adv. Anal. Steel Frames*, **1994**, 259-320.
- De Souza, R.M. (2000), *Force-based finite element for large displacement inelastic analysis of frames*, Ph.D. Dissertation, University of California, Berkeley.
- Duan, L., Loh, J. and Chen, W.F. (1993), “Moment-curvature relationships for dented tubular sections”, *J. Struct. Eng.*, **119**(3), 809-830.
- El-Tawil, S. and Deierlein, G.G. (1999), “Strength and ductility of concrete encased composite columns”, *J. Struct. Eng.*, **125**(9), 1009-1019.
- Fukumoto, Y. (1963), Moment-curvature-thrust program for wide-flange shapes, Report No. 205A.37; Fritz Engineering Lab.
- Gayathri, V., Shanmugam, N.E. and Choo, Y.S. (2004), “Concrete-filled tubular columns: Part 1 — Cross-section analysis”, *Int. J. Struct. Stab. Dynam.*, **4**(4), 459-478.
- Hsu, T.M. (1966), “Determination of the moment-curvature relation for a beam of nonlinear material”, Masters Thesis, University of Arizona, Tucson.
- Jiang, X.M., Chen, H. and Liew, J.R. (2002), “Spread-of-plasticity analysis of three-dimensional steel frames”, *J. Constr. Steel Res.*, **58**(2), 193-212.
- Kwak, H.G. and Kim, S.P. (2002), “Nonlinear analysis of RC beams based on moment-curvature relation”, *Comput. Struct.*, **80**(7-8), 615-628.
- Li, T.J., Liu, S.W. and Chan, S.L. (2015), “Cross-sectional analysis of arbitrary sections allowing for residual stresses”, *Steel Compos. Struct.*, **18**(4), 985-1000.
- Liu, S.W., Liu, Y.P. and Chan, S.L. (2012), “Advanced analysis of hybrid steel and concrete frames: Part I: Cross-section analysis technique and second-order analysis”, *J. Constr. Steel Res.*, **70**: 326-336.
- Monti, G. and Petrone, F. (2015), “Yield and ultimate moment and curvature closed-form equations for reinforced concrete sections”, *ACI Struct. J.*, **112**(4), 463.
- Neuenhofer, A. and Filippou, F.C. (1997), “Evaluation of nonlinear frame finite-element models”, *J. Struct. Eng.*, **123**(7), 958-966.
- Neuenhofer, A. and Filippou, F.C. (1998), “Geometrically nonlinear flexibility-based frame finite element”, *J. Struct. Eng.*, **124**(6), 704-711.
- Ngo-Huu, C. and Kim, S.E. (2012), “Practical nonlinear analysis of steel-concrete composite frames using fiber-hinge method”, *J. Constr. Steel Res.*, **74**, 90-97.
- Niceno, B. (2002), “Easymesh: a two-dimensional quality mesh generator”, *CP/OLJ*. <http://www.dinma.univ.trieste.it/nirftc/research/easymesh>.
- Oller, S. and Barbat, A.H. (2006), “Moment-curvature damage model for bridges subjected to seismic loads”, *Comput. Method. Appl. M.*, **195**(33-36), 4490-4511.
- Sato, T., Shimada, I. and Kobayashi, H. (2002), “A simple numerical method for biaxial bending moment-curvature relations of reinforced concrete column sections”, *Memoirs of the Faculty of Engineering, Osaka City University*, **43**, 59-67.
- Simão, P.D., Barros, H., Ferreira, C.C. and Marques, T. (2016), “Closed-form moment-curvature relations for reinforced concrete cross sections under bending moment and axial force”, *Eng. Struct.*, **129**, 67-80.
- Soranakom, C. and Mobasher, B. (2007), “Closed-form moment-curvature expressions for homogenized fiber-reinforced concrete”, *ACI Mater. J.*, **104**(4), 351.
- Spacone, E., Filippou, F.C. and Taucer, F.F. (1996), “Fibre beam-column model for non-linear analysis of R/C frames: Part I. formulation”, *Earthq. Eng. Struct. D.*, **25**(7), 711-726.

- Spacone, E., Filippou, F.C. and Taucer, F.F. (1996), "Fibre beam-column model for non-linear analysis of R/C frames: Part II. Applications", *Earthq. Eng. Struct. D.*, **25**(7), 727-742.
- Teh, L.H. and Clarke, M.J. (1999), "Plastic-zone analysis of 3D steel frames using beam elements", *J. Struct. Eng.*, **125**(11), 1328-1337.
- The European Committee for Standardization (CEN) (2004), *Eurocode 2: Design of Concrete Structures: Part 1-1: General Rules and Rules for Buildings*.
- Uy, B. (2001), "Strength of short concrete filled high strength steel box columns", *J. Constr. Steel Res.*, **57**(2), 113-134.
- Varma, A.H., Ricles, J.M., Sause, R. and Lu, L.W. (2002), "Seismic behavior and modeling of high-strength composite concrete-filled steel tube (CFT) beam-columns", *J. Constr. Steel Res.*, **58**(5), 725-758.

DL